The Structure, Cation Binding, Transport, and Conductance of Gly_{15}-Gramicidin A Incorporated into SDS Micelles and PC/PG Vesicles[†,‡]

S. S. Sham,[§,||] S. Shobana,[⊥] L. E. Townsley,[§,#] J. B. Jordan,[§] J. Q. Fernandez,[§,£] O. S. Andersen,[⊥] D. V. Greathouse,[§] and J. F. Hinton*[,§]

Department of Chemistry and Biochemistry, University of Arkansas, Fayetteville, Arkansas 72701, and Department of Physiology and Biophysics, Cornell University, Weill Medical College, New York, New York 10021

Received June 21, 2002; Revised Manuscript Received November 26, 2002

ABSTRACT: To further investigate the effect of single amino acid substitution on the structure and function of the gramicidin channel, an analogue of gramicidin A (GA) has been synthesized in which Trp_{15} is replaced by Gly in the critical aqueous interface and cation binding region. The structure of Gly_{15}-GA incorporated into SDS micelles has been determined using a combination of 2D-NMR spectroscopy and molecular modeling. Like the parent GA, Gly_{15}-GA forms a dimeric channel composed of two single-stranded, right-handed $\beta^{6.3}$-helices joined by hydrogen bonds between their N-termini. The replacement of Trp_{15} by Gly does not have a significant effect on backbone structure or side chain conformations with the exception of Trp_{11} in which the indole ring is rotated away from the channel axis. Measurement of the equilibrium binding constants and ΔG for the binding of monovalent cations to GA and Gly_{15}-GA channels incorporated into PC vesicles using ^{205}Tl NMR spectroscopy shows that monovalent cations bind much more weakly to the Gly_{15}-GA channel entrance than to GA channels. Utilizing the magnetization inversion transfer NMR technique, the transport of Na^+ ions through GA and Gly_{15}-GA channels incorporated into PC/PG vesicles has been investigated. The Gly_{15} substitution produces an increase in the activation enthalpy of transport and thus a significant decrease in the transport rate of the Na^+ ion is observed. The single-channel appearances show that the conducting channels have a single, well-defined structure. Consistent with the NMR results, the single-channel conductances are reduced by 30% and the lifetimes by 70%. It is concluded that the decrease in cation binding, transport, and conductance in Gly_{15}-GA results from the removal of the Trp_{15} dipole and, to a lesser extent, the change in orientation of Trp_{11}.

The role played by tryptophan residues in determining the properties of integral membrane proteins has been the subject of much interest (*1*, *2*). Within the lipid bilayer, the tryptophan residues tend to be asymmetrically located, clustering at the interface between the polar headgroup region and the hydrophobic interior in a relatively uniform layer just below the surface. This suggests a possible structural role for tryptophan residues in transmembrane sheets and helices, where they may play a part in the stabilization of the transmembrane segments and perhaps in the orientation and bilayer insertion process. The inherent dipolar nature and ability to form hydrogen bonds are thought to be the properties of the tryptophan residue responsible for this structural role. Furthermore, in proteins and peptides that act as transmembrane ion transporting channels, the tryptophan residues can affect the binding and transport of cations through ion−dipole interactions. The strategically located tryptophan residues at the aqueous interface initiate the transport process by enhancing capture and stabilizing the ion in the channel.

Because of the difficulty in obtaining high-resolution structural information for the very large protein channel systems, smaller model channel systems have been studied to obtain structure/function information that could relate to the large protein channels. Gramicidin A (GA),[1] a 15 residue polypeptide that forms monovalent cation specific channels in model membranes, has been found to have structural features in common with other ion channels (*3*−*6*). The three major, naturally occurring gramicidin species (A, B and C) have the amino sequence formyl-L-Val_1-D-Gly_2-L-Ala_3-D-Leu_4-L-Ala_5-D-Val_6-L-Val_7-D-Val_8-L-Trp_9-D-Leu_{10}-L-Xxx_{11}-D-Leu_{12}-L-Trp_{13}-D-Leu_{14}-L-Trp_{15}-ethanolamine, where Xxx is Trp in GA, Phe in GB, and Tyr in GC (*7*). The channels formed by GA, GB, and GC are composed of two single-

[†] Funding for this project was provided by NSF Grant MCB-9313835, NIH Grant 5P20RR15569-01, and NIH Grant GM21342 (OSA).

[‡] Coordinates for Gly_{15}-Gramicidin A have been deposited in the RCSB Protein Data Bank with accession code

* Corresponding author. e-mail: jhinton@uark.edu; phone: (501) 575-5143; fax: (501) 575-4049.

[§] University of Arkansas.

[||] Present address: Department of Chemistry, University of California, Davis, CA 95617.

[⊥] Cornell University.

[#] Present address: Department of Chemistry and Biochemistry, University of California, Santa Barbara, CA 93106

[£] Present address: Department of Natural Sciences, University of Guam.

[1] Abbreviations: GA, gramicidin A; Gly_{15}-GA, Gly_{15}-gramicidin A; d_2-TFE, deuterated trifluoroethanol (CF_3CD_2OH); d_{25}−SDS, deuterated sodium dodecyl sulfate; PC, L-α-phosphatidylcholine; PG, L-α-phosphatidylglycerol; DPhPC, diphytanoylphosphatidylcholine; LUV, large unilamellar vesicle; NMR nuclear magnetic resonance; DQF-COSY, double quantum filtered correlation spectroscopy; TOCSY, total correlation spectroscopy; NOESY, nuclear Overhauser spectroscopy; DG/SA, distance geometry/simulated annealing; ETA, ethanolamine.

10.1021/bi0204286 CCC: $25.00
Published on Web 01/23/2003

stranded, right-handed $\beta^{6.3}$-helices, joined by hydrogen bonds between their N-termini (*8*, *9*). Of the 15 residues in GA, four are tryptophans that are located at, or near, the aqueous interface at positions 9, 11, 13, and 15. These tryptophan residues are important in the insertion, folding, structure, and function of the GA channel (*10*). The structures of GA, GB, and GC are practically the same (*5*); however, the single-channel conductances (with Na^+ as the permeant ion) for the three channels differ (GA > GC > GB) (*11*, *12*). There have been many other single channel conductance studies on GA analogues in which the tryptophan residues are replaced by residues that have less polar and more polar side chains (*3* and references therein). In general, it is the position of substitution (i.e., 9, 11, 13, or 15), orientation, and magnitude of the dipole moment of the side chain that determines the effect on conductance. One must determine the complete structure of the gramicidin channel to define the relative orientations of the side chains since near (e.g., *i*, *i*+1) and far (e.g., *i*, *i*+6) interactions are important within the helix.

To determine the effect of tryptophan replacement on the structure and function of the GA channel, we have completed a systematic investigation for a synthetic analogue of GA in which Trp_{15} is replaced by glycine (Gly_{15}-GA). The 3D structure of this analogue incorporated into sodium dodecyl sulfate micelles, including backbone configuration and side chain orientations for the full dimer channel, has been determined by the combination of NOESY derived distance constraints and molecular modeling. For Gly_{15}-GA channels incorporated into vesicles, the thermodynamic parameters for cation binding at the channel entrance have been determined using $^{205}Tl^+$ NMR spectroscopy (*13*−*15*), and the activation enthalpy for cation transport has been determined using the magnetization inversion transfer NMR technique (*16*). We present here a comparison of the structure and transport properties of Gly_{15}-GA with those previously reported for GA (*5*, *13*−*16*). We also examined the properties of Gly_{15}-GA channels electrophysiologically. These results are in overall agreement with the NMR results.

EXPERIMENTAL PROCEDURES

Materials. Gly_{15}-GA was obtained using an Applied Biosystems 431A Peptide Synthesizer (Foster City, CA). The amino acid sequence of the Gly_{15}-GA analogue was checked with an Applied Biosystems 473A Protein Sequencer (Foster City, CA). Two HPLC runs were used to purify the analogue. The purity of the analogue (>98%) was assessed using electrospray ionizaton mass spectrometry (Mass Consortium, San Diego, CA and the University of Arkansas Mass Spectrometry Center). Circular dichroism spectra were obtained with a Jasco J-710 Spectropolarimeter (Jasco, Inc., Easton, MD). The ^1H and ^{23}Na NMR spectra were obtained with a Varian VXR 500S spectrometer (Varian, Inc., Palo Alto, CA). The ^{205}Tl NMR spectra were obtained with a JEOL FX 90Q spectrometer (JEOL USA, Peabody, MA).

Deuterated sodium dodecyl sulfate (d_{25}-SDS), deuterium oxide (D_2O), and deuterated trifluoroethanol (CF_3CD_2OH, d_2-TFE) were obtained from Cambridge Isotope Laboratories (Cambridge, MA). The d_{25}-SDS was recrystallized twice from 95% ethanol. $TlNO_3$ (Alfa Products, Morton Thiokol Inc., Danver, MA) was recrystallized twice from distilled water and dried to a constant weight at 90 °C, 40 mm Hg. A 100 mM phosphate buffer solution, pH 6.5, was purchased from PGC Scientifics (Gaithersburg, MD). L-α-Phosphatidylcholine (PC) from frozen egg yolk (100 mg/mL in chloroform) was obtained from Sigma Chemical Company (Saint Louis, MO). L-α-Phosphatidylglycerol (PG) (sodium salt, 25 mg/mL in 90% chloroform/10% methanol) was purchased from Avanti Polar Lipids Company (Birmingham, AL). Dysprosium (III) nitrate, $Dy(NO_3)_3$, was obtained from Alfa Aesar (Ward Hill, MA). Sodium tripolyphosphate, $Na_3P_3O_{10}$, was purchased from Aldrich Chemical Co. (Milwaukee, WI).

The sample of Gly_{15}-GA incorporated into d_{25}−SDS micelles used for the ^1H 2D-NMR experiments was prepared in the following manner (*6*). A 50 mM solution of the analogue dissolved in d_2-TFE was combined with 275 mM aqueous d_{25}-SDS solution (89% pH 6.5 buffer/11% D_2O, v/v) to a final concentration of approximately 5 mM Gly_{15}-GA and 250 mM d_{25}-SDS in 80% pH 6.5 buffer/10% D_2O/10% d_2-TFE. The sample was then sonicated (low power) for 5 min to facilitate incorporation of Gly_{15}-GA into the d_{25}-SDS micelles.

For the monovalent cation binding studies, Gly_{15}-GA was incorporated into PC vesicles using the method of Urry et al. (*15*, *17*−*21*). The CD spectrum of Gly_{15}-GA incorporated into PC vesicles was the same as that of GA incorporated into PC vesicles. It has been shown that the CD spectrum of GA incorporated into PC vesicles represents the $\beta^{6.3}$-helical channel state (*13*−*15*, *17*, *19*−*25*). For the $^{205}Tl^+$ ion binding studies, in the absence of Na^+ or K^+, samples were prepared to have 5 mM Gly_{15}-GA dimer, 100 mM PC, and varying Tl^+ concentrations (0.05−0.5 mM) (*19*, *20*). Samples used for the Na^+ and K^+ competition binding studies contained 5 mM Gly_{15}-GA dimer, 100 mM PC, 15 mM $TlNO_3$, and varying concentrations of $NaNO_3$ or KNO_3 (0.1−0.4 M) (*14*, *15*, *19*, *20*).

The magnetization inversion transfer experiments required the synthesis of a $^{23}Na^+$ chemical shift reagent and preparation of large unilamellar vesicles (LUV). The $^{23}Na^+$ chemical shift reagent, $Na_7Dy(P_3O_{10})_2$, was prepared by the reaction between $Dy(NO_3)_3$ and $Na_5P_2O_{10}$, as previously described (*26*−*28*). The method of reverse phase ether evaporation was used to prepare LUV (*16*, *29*−*31*) composed of a mixture of PC:PG in a 4:1 mole ratio. This method gave a high Na^+ encapsulation (∼30%) in the inner aqueous solution. Incorporation of Gly_{15}-GA into the LUV (*6*, *30*, *31*) was achieved by the addition of a small amount of Gly_{15}-GA dissolved in TFE to the vesicle solution followed by agitation with a vortex mixer. The solution was then incubated for 3 h at 65 °C. After cooling to room temperature, a small amount of D_2O was added to the sample. Finally, the LUV solution was diluted 1:1 with the chemical shift reagent bringing the final concentrations of Gly_{15}-GA, chemical shift reagent and Na^+ to 2, 5, and 100 mM, respectively. The $^{23}Na^+$ chemical shift reagent is membrane-impermeable, thus the final concentration refers only to the aqueous environment outside of the LUV, whereas the Na^+ achieves an osmotic balance between the inner and outer aqueous pools. The chemical shift difference between the inner and outer $^{23}Na^+$ is approximately 2000 Hz. Figure 1 shows the $^{23}Na^+$ NMR spectrum for a sample made with Gly_{15}-GA channels.

When performing cation binding and transport studies, one assumes that a single helical form of gramicidin is present

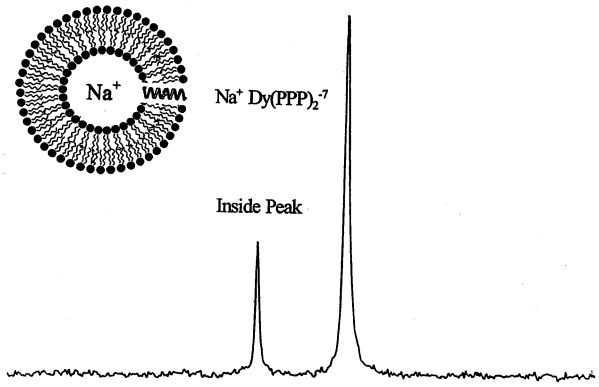

FIGURE 1: ^{23}Na NMR spectrum of the sodium ions inside of the vesicles (smaller signal on the left) and the sodium ions on the outside of the vesicles in contact with the shift reagent (larger signal on the right).

in vesicles. While this appears to be true for GA and some analogues, it has been shown that a number of others form multiple helical species in SDS micelles (*32*−*34*), and one would assume in vesicles and bilayers also. Cation binding and transport studies performed in the presence of multiple helical forms would be difficult to interpret. 1- and 2D ^1H NMR techniques have been developed to detect the presence of multiple helical forms of gramicidin analogues incorporated into SDS micelles (*32*−*34*). Using these techniques, we have confirmed that only one helical form exists for Gly_{15}-GA incorporated into SDS micelles.

METHODS

2D-NMR Spectroscopy and Molecular Modeling. All 2D-NMR experiments were performed using a Varian VXR 500S NMR spectrometer. The ^1H chemical shifts were determined using the standard technique involving DQF-COSY, TOCSY, and NOESY experiments (*35*). A spectral width of 6000 Hz was used in both dimensions for each 2D experiment. All spectra were recorded at 55 °C in the phase-sensitive mode (*36*) using the States, Ruben, and Haberkorn method (*37*). Water suppression was achieved by transmitter presaturation.

The DQF-COSY spectrum was acquired in 512 t_1 increments with 8192 or 16384 t_2 data points to achieve high digital resolution. One hundred twenty-eight transients were used per t_1 increment.

The TOCSY spectrum was acquired in 256 t_1 increments (64 transients/increment) with 4096 t_2 data points. The data for these experiments were acquired with a mixing time of 75 ms using the MLEV-17 mixing scheme (*38*).

The NOESY spectrum was acquired in 512 t_1 increments (128 transients/increment) with 8192 t_2 data points. A delay of 2.7 s was used before the initiation of the pulse sequence. A mixing time of 40 ms was used to ensure that cross-peak volumes were within the linear region of NOE buildup.

The molecular modeling strategy (including generation of distance constraints, DG/SA, relaxation matrix calculations, and minimization) for the determination of the 3D structure of the Gly_{15}-GA dimer channel is the same as that used in our previous determination of the structure of GA (6), thus making direct comparison of these analogues meaningful. The dimer structure of Gly_{15}-GA was modeled using a total of 13 hydrogen bonds (3 monomer−monomer connections) and 530 NOESY-derived distance constraints (27 monomer−monomer interactions). The root-mean-square-deviations (RMSD) between the structures of GA and Gly_{15}-GA are 1.53 for all atoms except those of residue 15 and the ethanolamine and 1.01 for all heavy atoms except those of residue 15 and ethanolamine. Residue 15 was removed from the comparison because the residue at this position is different. The ethanolamine was removed from the comparison because it has a large degree of motional freedom at the aqueous end of the channel. A value of 0.53 was obtained for all backbone atoms.

^{205}Tl NMR Spectroscopy. The Tl^+ ion is a convenient and relevant ion for the study of the equilibrium binding to the gramicidin channel because of the following: (1) The Tl^+ ion is transported through the channel. The ionic radius of the Tl^+ ion is intermediate between Na^+ and Cs^+, which are also transported through the channel. (2) The Tl^+ ion is more tightly bound to the channel than are the alkali cations. The tighter binding to the channel means the equilibrium binding constant can be determined with higher precision. (3) Thallium is particularly well suited for the NMR experiment because of its intrinsic nuclear properties. Thallium has two isotopes, ^{203}Tl (29.5% natural abundance) and ^{205}Tl (70.5% natural abundance), which have spin $I = {}^1/_2$. The relative receptivity of ^{205}Tl is 0.1355 with respect to the proton with an assigned value of 1. This makes ^{205}Tl the fourth most receptive spin $^1/_2$ nuclide. Not only are the thallium isotopes relatively easy to observe in the NMR experiment, the spectral parameters of chemical shift, coupling constant, and spin lattice relaxation time are exceptionally sensitive to the chemical (i.e., electronic) environment in which the thallium nucleus is placed (*39*). ^{205}Tl NMR spectroscopy (i.e., the chemical shift) provides an excellent probe of the environment about the Tl^+ ion; therefore, the equilibrium between free and gramicidin bound Tl^+ can be measured with high precision.

The equilibrium constant (K_{eq}) for the binding of the Tl^+ ion to the gramicidin channel is determined from a theoretical analysis of the relationship between $^{205}Tl^+$ chemical shift and Tl^+ concentration in the presence of a constant concentration of Gly_{15}-GA incorporated into lipid vesicles. The value of ΔG for the cation binding process is derived from the relationship between K_{eq} and temperature ($\Delta G = -RT \ln K_{eq}$). Details of this technique and the analysis of the chemical shift data have been published previously (*15*). The competition binding-^{205}Tl NMR technique used to determine the equilibrium binding constants for the Na^+ and K^+ have been described in detail in previous papers (*14*, *20*). This technique involves measuring the $^{205}Tl^+$ chemical shift, in the presence of constant Tl^+ concentration and constant concentration of Gly_{15}-GA incorporated into the lipid vesicles, as a function of the concentration of competing Na^+ or K^+.

Magnetization Inversion Transfer. The magnetization inversion transfer technique (*16*, *40*−*52*) was used to determine the rates and rate constants for the transport of Na^+ through Gly_{15}-GA and GA channels incorporated into PC/PG vesicles. The magnetization inversion transfer pulse sequence [$90_x° - t_1 - 90_x° - t_{mix} - 90_x° -$ acquire(t_2)] consists of three nonselective $(\pi/2)_x$ pulses with the transmitter frequency placed on the desired frequency to be labeled (i.e., the signal corresponding to the outer pool of $^{23}Na^+$ ions). The interval between the first two pulses, t_1, is equal to one-half of the reciprocal of the chemical shift difference between

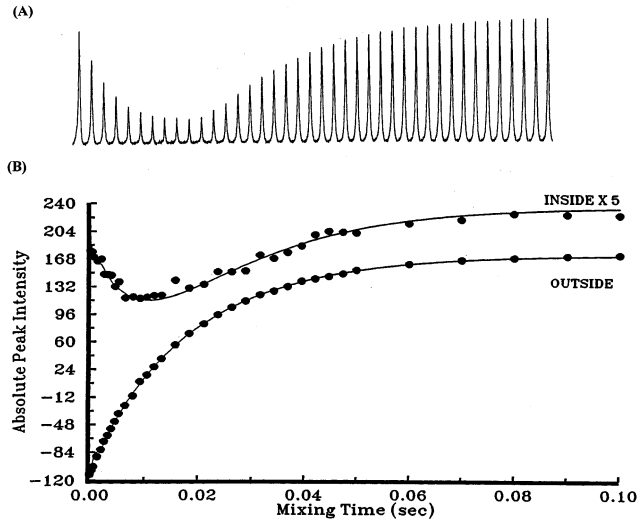

FIGURE 2: (A) The ^{23}Na NMR signal of the sodium ions on the inside of the vesicles as a function of mixing time increasing from the left to the right. (B) The theoretical fit of the inside and outside ^{23}Na NMR signals as a function of mixing time. The filled circles are experimental data. The solid lines are computer fits of the experimental data.

the inner and outer $^{23}Na^+$ signals. This chemical shift difference must be made as large as possible since the value of t_1 has to be considerably shorter than the T_1 of the two exchanging sites. A total of 25−30 mixing times were used at each of the nine temperatures for which the data were collected. The nature of the experiment is such that at short mixing times, some of the inverted outside $^{23}Na^+$ signal is transferred to the inner aqueous $^{23}Na^+$ pool of the vesicle by the mechanism of ion transport through the gramicidin channel. This causes a decrease in the signal intensity of the inner $^{23}Na^+$ NMR signal. The inner $^{23}Na^+$ NMR signal for a typical magnetization inversion transfer experiment is shown for Gly_{15}-GA in Figure 2A. The magnetization inversion transfer data were analyzed using the method of Muhandiram and McClung (*53*) with the CIFIT computer program of Bain et al. (*54*−*56*), shown in Figure 2B, to determine rates, rate constants and the activation enthalpy of Na^+ transport.

Electrophysiology. Single-channel measurements were performed at 25 ± 1 °C using the bilayer punch method (57) in planar lipid bilayers formed from a solution of DPhPC in *n*-decane (2−2.5wt %/vol). The electrolyte solutions were unbuffered NaCl, KCl, or CsCl. Aliquots of Gly_{15}-GA dissolved in ethanol were added to the aqueous phases on both sides of the bilayer while stirring. In the heterodimer experiments, Gly15-GA and the reference GA were added either asymmetrically, to one side of the bilayer, or symmetrically, to both sides of the bilayer. The nominal aqueous concentration of Gly_{15}-GA varied between 10^{-12} and 10^{-11} M, similar to the concentration of GA. Curent signals were recorded using a Dagan 3900 Patch Clamp amplifier (Dagon Corporation, Minneapolis, MN), filtered with an 8-pole Bessel filter, and digitized at 5 times the filter frequency (*57*, *58*). The average channel lifetime (τ) was estimated by fitting single exponential distributions to the duration distributions. This was done using the equation $N(t) = N(0)\exp(-t/\tau)$, where $N(0)$ is the total number of channels and $N(t)$ denotes the number of channels with a duration longer than time t (*58*, *59*).

Table 1: $^{205}Tl^+$ Chemical Shifts as a Function of Tl^+ Activity at 307.15 K, Equilibrium Binding Constants (K_{eq}) for Tl^+ as a Function of Temperature, and the ΔG of Tl^+ Binding to Gly_{15}-GA and GA Channels Incorporated into PC Vesicles[a]

	Gly_{15}-GA	GA
Tl^+ activity ($\times 10^4$) activity = $\gamma[Tl^+]$	$^{205}Tl^+$ chemical shift (Hz)	$^{205}Tl^+$ chemical shift (Hz)
4.87	535	3712
9.65	496	3476
19.02	432	3078
37.32	374	2504
46.30	369	2198
55.19	344	1964
72.75	322	1663
90.04	295	1431
123.34	256	1029
173.60	215	790
214.03	198	666
253.75	166	554
331.47	149	424
407.31	122	338
temperature (K)	K_{eq} (M^{-1})	K_{eq} (M^{-1})
303.15	138.2	
307.15	113.0	506
310.15	104.8	457
313.15	78.1	424
317.15	57.8	363
325.15	38.8	259
$\Delta G_{307.15K}$ (kcal/mol)	-2.9 ± 0.1	-3.8 ± 0.5

[a] Sample concentrations: 5 mM Gly_{15}-GA or GA dimer; 100 mM PC.

RESULTS AND DISCUSSION

The transport of a monovalent cation through the gramicidin channel involves five steps (60): (1) diffusion through water to the entrance of the channel; (2) binding to the channel entrance; (3) movement through the channel; (4) interaction with the binding site at the opposite end of the symmetric dimer channel; (5) diffusion away from the channel. The binding step involves the removal of some of the water molecules from the hydration sphere of the cation replacing them with backbone carbonyl oxygen atoms that line the channel. This is an equilibrium binding process, and the equilibrium constants for Na^+, K^+, and Tl^+ have been measured using the $^{205}Tl^+$ chemical shift technique. Table 1 contains the $^{205}Tl^+$ chemical shift data at 307.15 K, equilibrium binding constants (K_{eq}) and $\Delta G_{307.15K}$ for Tl^+ binding to Gly_{15}-GA and GA channels. Table 2 presents the results from the Na^+ and K^+ competition binding experiments: $^{205}Tl^+$ chemical shifts as a function of Na^+ and K^+ activity at 317.15 K, equilibrium binding constants (K_{eq}) and $\Delta G_{307.15K}$ for the binding of Na^+ and K^+ to Gly_{15}-GA and GA channels. The kinetics of ion transport through the gramicidin channel, related to steps 2−4, have been determined using the magnetization inversion transfer technique. Rates, rate constants, and the activation enthalpies of Na^+ transport through the Gly_{15}-GA and GA channels are shown in Table 3.

The relative ease with which GA can be modified by single amino acid replacement provides the opportunity to investigate how changes in side chain polarity affect the 3D structure of the channel, as well as cation binding and transport. The replacement of the tryptophan residue at position 15, which is at the aqueous interface, with glycine reduces the size of the side chain at that position and removes

Table 2: $^{205}Tl^+$ Chemical Shifts as a Function of Na^+ or K^+ Activity at 317.15 K in the Presence of Gly_{15}-GA Channels Incorporated into PC Vesicles[a]

Na^+ activity ($\times 10^2$) activity $= \gamma[Na^+]$	$^{205}Tl^+$ chemical shift (Hz)	K^+ activity ($\times 10^2$) activity $= \gamma[K^+]$	$^{205}Tl^+$ chemical shift (Hz)
7.58	192.9	7.33	195.3
10.95	190.4	10.44	173.3
14.40	163.6	13.18	168.5
17.10	173.3	15.82	163.6
19.90	158.7	18.21	151.4
25.60	156.2	22.96	124.5

temperature (K)	Gly15-GA K_{eq} (M^{-1})		GA K_{eq} (M^{-1})	
	Na^+	K^+	Na^+	K^+
307.15	6.4	12.6	31.6	54.2
310.15	5.6	13.1	29.4	49.6
313.15	5.0	7.6	27.2	43.3
317.15	3.8	7.2	23.4	39.9
$\Delta G_{307.15K}$ (kcal/mol)	-1.1 ± 0.1	-1.6 ± 0.1	-2.1 ± 0.1	-2.4 ± 0.1

[a] Equilibrium binding constants (K_{eq}) as a function of temperature, and the ΔG of binding for Na^+ and K^+ to Gly_{15}-GA and GA channels incorporated into PC Vesicles. Sample concentrations: 5 mM Gly_{15}-GA or GA dimer; 100 mM PC; 15 mM Tl^+.

Table 3: Rates, Rate Constants, and Activation Enthalpy ($\Delta H^{\ddagger}$) for the Transport of Na^+ through Gly_{15}-GA and GA Channels Incorporated into PC/PG Vesicles[a]

temperature (K)	Gly_{15}-GA rate (s^{-1})	Gly_{15}-GA rate constant, $k \times 10^{13}$ ($mL^2\ s^{-1}\ mol^{-1}$)	GA rate (s^{-1})	GA rate constant, $k \times 10^{13}$ ($mL^2\ s^{-1}\ mol^{-1}$)
287.93	53.29	9.07	141.17	26.00
290.60	63.99	10.83	158.69	29.24
293.33	76.08	12.84	172.17	31.82
296.09	86.18	14.62	187.27	34.84
298.88	99.01	16.74	204.25	38.44
301.89	109.87	18.70	223.33	42.79
304.61	123.12	21.24	235.95	46.00
307.36	132.34	23.32	249.73	50.03
310.25	140.37	25.43	271.76	56.14
$\Delta H^{\ddagger}$ (kcal/mol)	7.5 ± 0.2		5.4 ± 0.3	

[a] Sample concentrations: 2 mM Gly_{15}-GA; PC:PG mole ratio of 4:1; 100 mM Na^+.

a critical dipole from the channel entrance. The capture and binding of a cation at the channel entrance is primarily the result of the interaction between the ion and the carbonyl oxygen; however, this is modulated by the long-range ion-tryptophan dipole interaction. Removal of the tryptophan side chain at the channel entrance would be expected to reduce the strength of the binding interaction. This is what we observe with the $^{205}Tl^+$ chemical shifts, the equilibrium binding constants and the $\Delta G_{307.15K}$ of binding for Tl^+, Na^+, and K^+ with Gly_{15}-GA (see Tables 1 and 2). In Table 1 it can be seen that the $^{205}Tl^+$ chemical shift is much less with Gly_{15}-GA than with GA, indicating weaker binding with Gly_{15}-GA. The equilibrium binding constants are less for Tl^+, Na^+, and K^+ with Gly_{15}-GA than with GA, and the values of $\Delta G_{307.15K}$ for these ions also indicate weaker binding to Gly_{15}-GA. The rates, rate constants, and activation enthalpies for the transport of Na^+ ions through the Gly_{15}-GA and GA channels are shown in Table 3. Obviously, with decreased rates and rate constants and an increased activation enthalpy,

Table 4: Channel Characteristics of Gly_{15}-GA and GA Channels in 1M NaCl, 1M KCl and 1M CsCl[a]

peptide	channel conductance (pS) 1 M NaCl	1 M KCl	1 M CsCl	channel duration (ms) 1 M NaCl	1 M KCl	1 M CsCl
Gly_{15}-GA	8.5	17.3	34.8	209	207	125
GA	15.0	27.5	46.4	680	743	674

[a] At +200 mV.

the movement of Na^+ ions through the Gly_{15}-GA channel is significantly slower than through the GA.

To discover if the slower movement of ions through the Gly_{15}-GA channel is solely the result of the removal of the tryptophan dipole or whether the removal of the tryptophan residue also changes the structure of the channel in such a manner as to diminish ion transport, we have determined the 3D structure, including backbone and side chain conformations, of Gly_{15}-GA. Figure 3 shows an overlay of the backbone, residues 1−8 and residues 9−15 of Gly_{15}-GA and GA. Like GA, the Gly_{15}-GA channel is composed of two single-strand, right-handed, $\beta^{6.3}$-helices joined by hydrogen bonds between their N-termini. The removal of Trp_{15} in Gly_{15}-GA creates a small difference in the backbone structure at the C-terminus near the ethanolamine (ETA). The other, notable difference between the two structures involves the orientation of the Trp_{11} side chain. In Gly_{15}-GA, the Trp_{11} side chain is oriented away from the channel axis, as shown in Figure 4. The cation binding site for GA has been identified as a "pocket" formed by residues 10−15 (*24*, *61*−*64*). The binding of a cation in this "pocket" involves the carbonyl oxygen atoms of the amino acid residues and the long-range ion−tryptophan dipole interactions. The position of the Trp_{11} dipole being further away from the channel axis may also contribute to the weaker cation binding for Gly_{15}-GA compared to GA. The importance of the ion-tryptophan dipole interaction on cation binding and transport has been investigated and reduction of the total dipole moment of the binding "pocket" by successive Trp → Phe substitutions does diminish the single-channel conductances of the gramicidin channel (*11*, *65*). This effect is directly related to the sequential loss of the indole ring dipoles, each of which promotes both cation entry and permeation due to the ion−dipole interaction. Conversely, the fluorination of the indole ring, which increases the dipole moment, has been found to increase the single-channel conductance (*66*−*69*).

As would be expected from the NMR results, which show only one major conformer, Gly_{15}-GA forms predominately one type of channel in DPhPC bilayers in both 1.0 M NaCl and KCl. Figure 5 shows results obtained with Na^+ and K^+ as permeant ions. Table 4 summarizes the results obtained with 1.0 M NaCl, KCl, and CsCl. For both Na^+ and K^+, the conductance of Gly_{15}-GA channels is reduced ≈30%, as compared to GA channels and the lifetimes are reduced by ≈70%.

Current−voltage characteristics ($i-V$ characteristics) of Gly_{15}-GA channels were determined using both Na^+ and K^+ as the permeant ions (at 0.5, 1, and 2M NaCl or KCl). Figure 6 shows the $i-V$ characteristics of Gly_{15}-GA channels as well as those of native GA channels. The $i-V$ characteristics of Gly_{15}-GA channels show similar trends to those of native GA channels, though the ion permeability is reduced in Gly_{15}-GA relative to native GA channels. The concentration

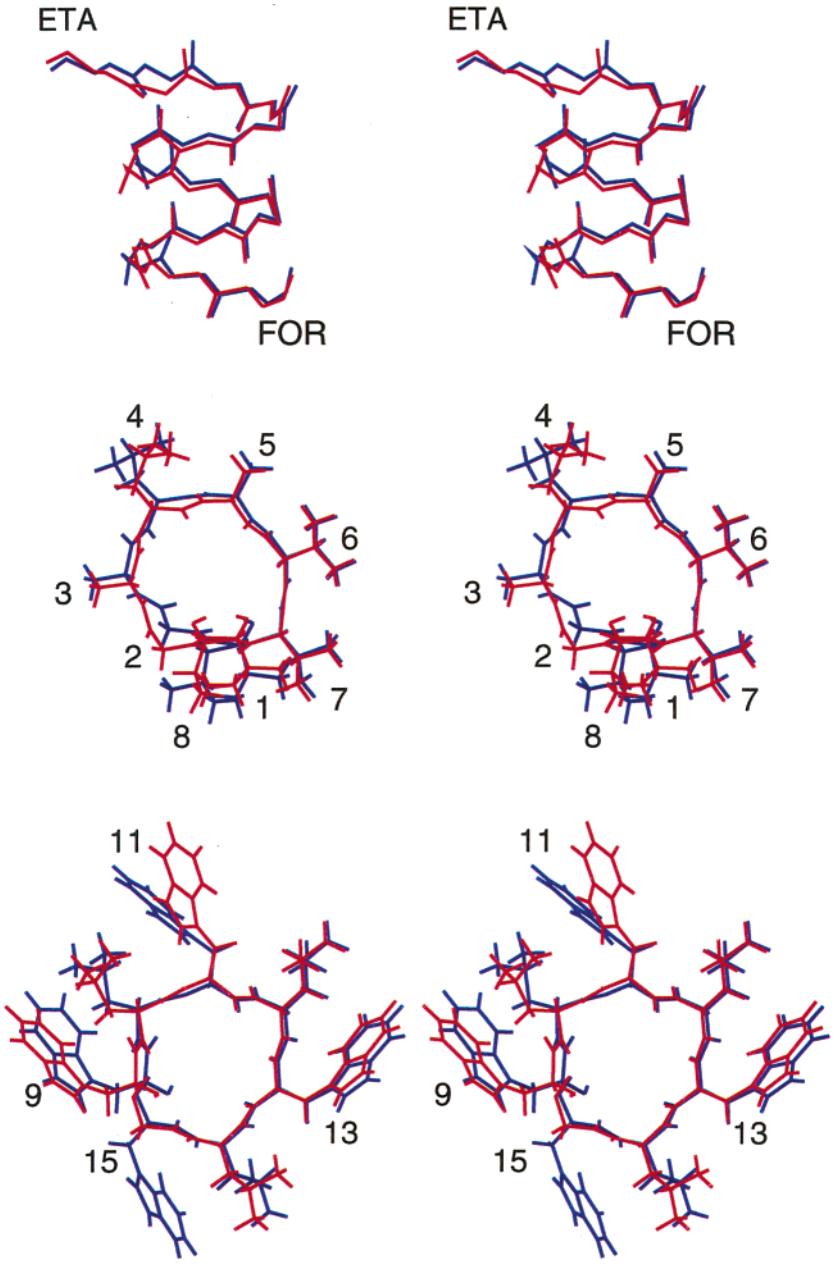

FIGURE 3: Divergent stereoviews showing the heavy-atom superposition of the final DISCOVER minimized structures of Gly_{15}-GA (red) and GA (blue). The top image is a side view showing the heavy atoms of the backbone, including formyl and ethanolamine capping groups, for one-half of the channel (monomer). The middle and bottom images are end-on views showing all atoms for residues Val_1 through D-Val_8 and residues Trp_9 through Trp_{15}, respectively. The formyl groups are aligned in all three figures.

dependence of the changes in $i-V$ characteristics is comparable for the two channel types.

The reduced conductance is in general agreement with the expectations from Trp → Phe substitutions (*65*), although the conductance change for Na^+ is larger than that observed with Trp → Phe substitution. The decrease in channel lifetime, however, is much larger than would have been expected from the Trp → Phe substitutions (*65*), which could indicate that the Trp residues' impact on channel function is the result of their having a dipole moment and their ability to form hydrogen bonds with acceptors at the bilayer/solution interface. The aromatic character of the side chain also may be important (*70*) in the sense that the planar aromatic ring might have favorable interactions with the interface, which would be consistent with the results of Wimley and White (*71*). It cannot be excluded, however, that the reorientation of Trp_{11} may be involved, as this would alter the electrostatic interactions between the permeant ions and the side chain dipoles. The aromatic residue at position 11 seems to be particularly important in terms of modulating channel function (*65*).

The reduced conductance is in general agreement with the reduced ion permeation rates deduced from the magnetization inversion transfer results (Figure 2 and Table 3) and could, in principle, result from changes in any of the rate constants describing the steps in ion permeation. To understand the basis for the reduced ion permeability of the Gly_{15}-GA channels, heterodimer experiments were performed in which GA was added to only one side of the bilayer (which is the electrical reference), whereas Gly_{15}-GA was added to each of the aqueous phases. At both +200 or −200 mV, two peaks were observed in the current transition amplitude histograms

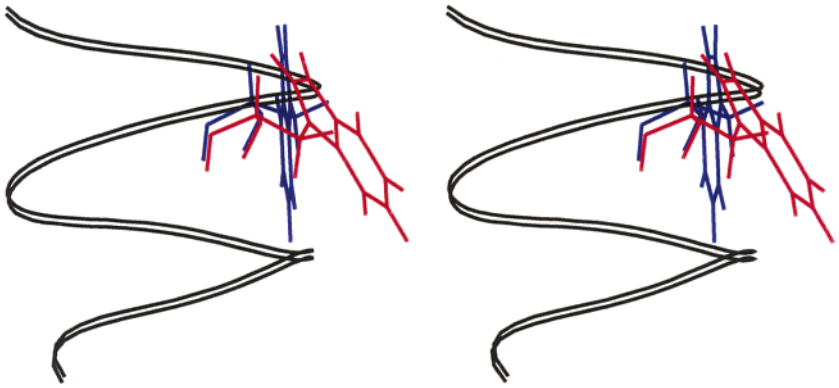

FIGURE 4: Divergent stereoview showing the orientation of the Trp_{11} side chains in Gly_{15}-GA (red) and GA (blue) with respect to the channel. To simplify visualization, only a monomer is shown, and the channel is represented by a two-thread ribbon.

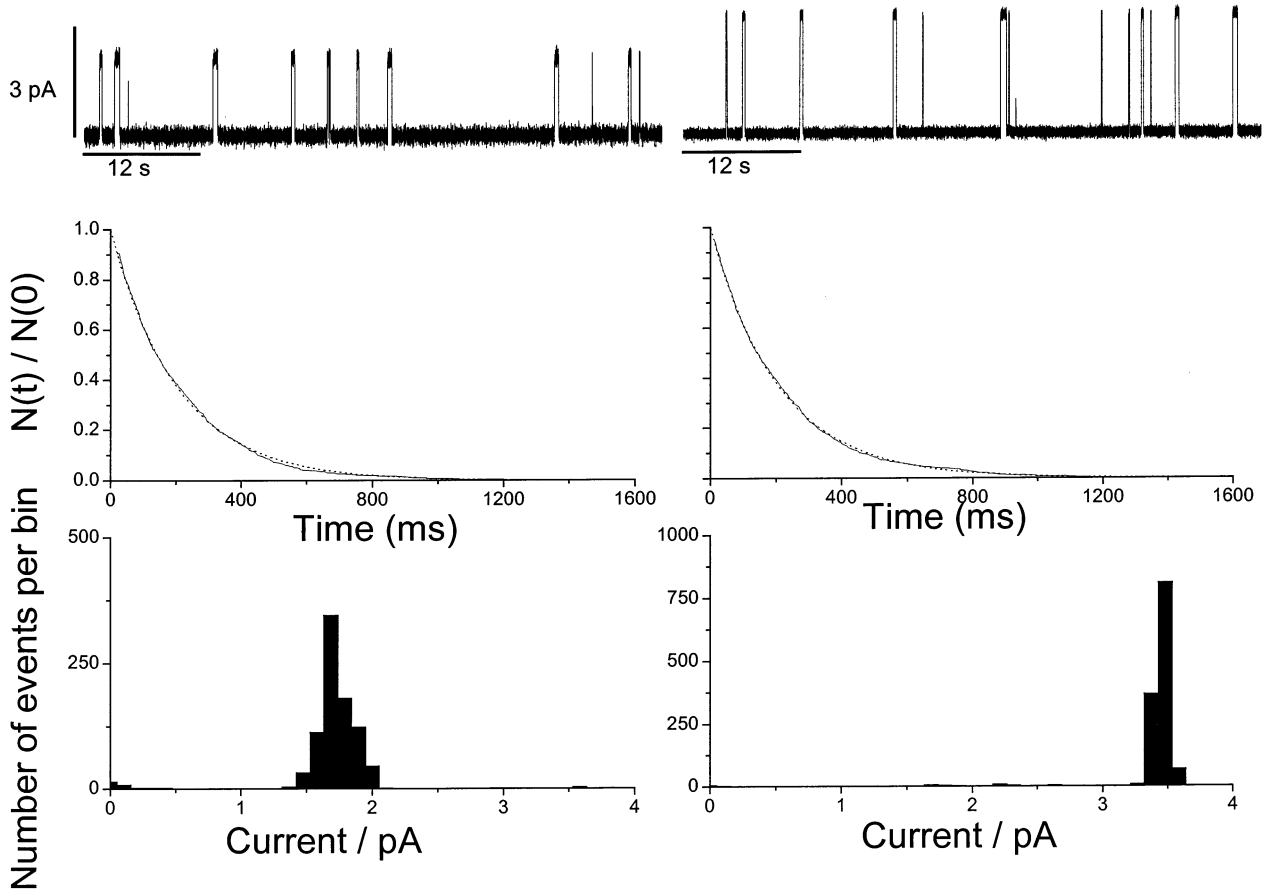

FIGURE 5: Single channel characteristics of Gly_{15}-GA in 1M NaCl (left panels) and 1 M KCl (right panels) solution. Top panels show one-min current traces, the middle panels show the normalized single-channel duration histograms (survivor plot plus the best single-exponential fit), and the bottom panels give the current transition amplitude histograms. The survivor plots are fitted with a single-exponential distribution $N(t)/N(0) = \exp(-t/\tau)$, where $N(0)$ is the total number of channels, $N(t)$ the number of channels with a duration longer than t, and τ the average channel lifetime. 1.0 M NaCl or KCl, 200 mV.

(Figure 7, top and middle panels): one representing homodimeric Gly_{15}-GA channels, where a Gly_{15}-GA monomer from one monolayer associates with a Gly_{15}-GA from the other monolayer, and a heterodimer peak, where a Gly_{15}-GA monomer from one monolayer associates with a GA monomer from the other monolayer. The different positions of the heterodimer peaks at +200 and −200 mV indicate that the energy barrier for the Gly_{15}-GA/GA heterodimeric channels is asymmetric, so that the permeating ions experience a different profile as they traverse the channels in the Gly_{15}-GA → GA and the GA → Gly_{15}-GA directions. The different current amplitudes taken together with the reduced ability of Na^+ and K^+ to displace Tl^+ in the channel (Table 2) suggest that a major reason for the reduced ion permeability is that the energy barrier for Na^+ entry into the Gly_{15}-GA subunit is higher than that for entry into the GA subunit (*65*, *72*).

The current transition histograms obtained when GA is added symmetrically to both chambers are given in the bottom panel of Figure 7. Four peaks were observed: two homodimeric peaks; one each for the Gly_{15}-GA and GA channels and two heterodimeric peaks; one each for GA/Gly_{15}-GA and Gly_{15}-GA/GA channels, corresponding to the different heterodimeric peaks in the asymmetric experiments

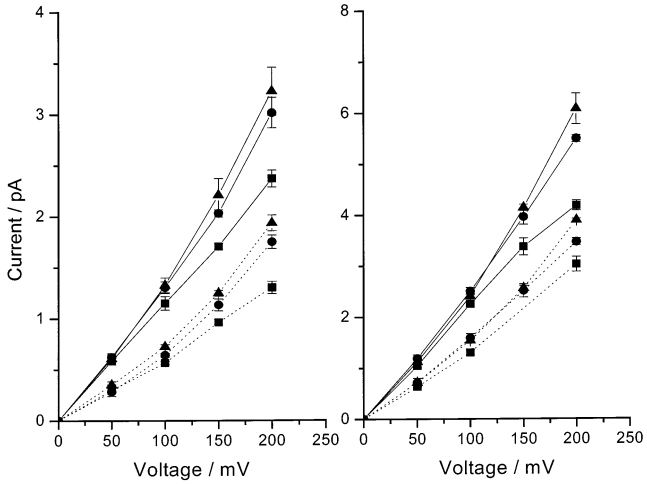

FIGURE 6: The current−voltage relationship ($i-V$) of Gly_{15}-GA channels (solid line and symbols) and GA channels (interrupted line and open symbols) in 1 M NaCl (left) and KCl (right). For each panel results were obtained at 0.5 (■), 1 (●), and 2 M (▲) NaCl or KCl.

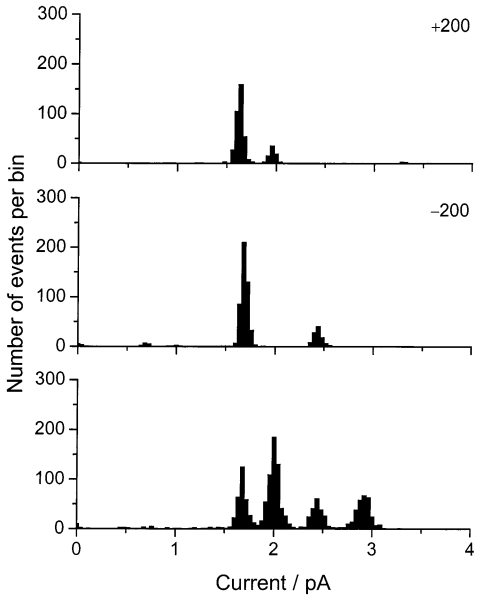

FIGURE 7: The current transition amplitude histograms obtained in heterodimer experiment with Gly_{15}-GA and GA in 1 M NaCl (200 mV). Gly_{15}-GA was added to both aqueous phases, whereas GA was added only to the front of the chamber. The top and middle panels show the results obtained under these asymmetric conditions, where the GA-containing solution is the electrical reference and the applied potential is +200 mV (current in the Gly_{15}-GA → GA direction) and −200 mV (current in the GA → Gly_{15}−GA direction), respectively. The bottom panel shows the current transition amplitudes when both GA and Gly_{15}-GA are present on both sides of the bilayer. The current transitions amplitudes for Gly_{15}-GA and GA homodimeric channels are 1.68 ± 0.05 and 2.91 ± 0.06 pA, respectively, and the currents for GA/Gly_{15}-GA and Gly_{15}-GA/GA heterodimeric channels are 2.00 ± 0.06 and 2.44 ± 0.05 pA.

in the top two panels. Though unnecessary in this case, where the channel structure is determined directly from the NMR results, the presence of heterodimers shows that Gly_{15}-GA channels are right-handed head-to-head $\beta^{6.3}$ helical dimers (*59*).

Given the importance of the Trp residues in determining the gramicidin channel folding (*73*), an investigation was made of whether Gly_{15}-GA could form heterodimers with

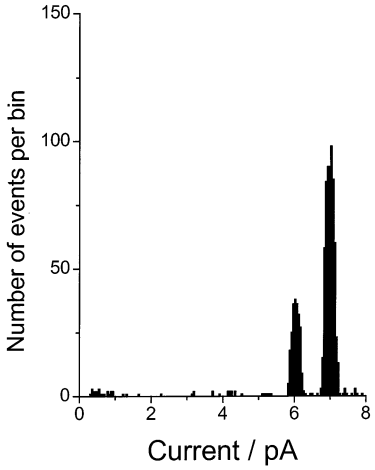

FIGURE 8: The current transition amplitude histograms obtained in heterodimer experiment with symmetric addition of Gly_{15}-GA and des-Val_1-GA^- in 1 M CsCl. There are total of 923 transitions, but only two peaks are seen in the histogram: one at ∼6 pA, representing des-Val_1-GA^- channels, with 231 transitions (25%), and one at ∼7 pA, representing Gly_{15}-GA channels, with 620 transitions (67%). Each of the major peaks represents a single channel type, as evident by their lifetime distributions (results not shown). We thus can account for 851, or 92% of the transitions, and no other peak encompasses more than 2% of the transitions, which indicates that heterodimers do not form between these two analogues. 1.0 M CsCl, 200 mV.

the des-Val_1-GA^- (an enantiomeric GA analogue in which the chirality of each residue in the sequence is shifted and D-Val_1 is deleted). Des-Val_1-GA^- forms only left-handed $\beta^{6.3}$-helical channels, which are terminated with an L-residue. Thus, if Gly_{15}-GA could form left-handed channels, they would present themselves as a distinct channel type in heterodimer experiments with des-Val^1-GA^-. To optimize channel detection, these experiments were performed with Cs^+ as the permeant ion. There was no evidence for heterodimers between Gly_{15}-GA and des-Val_1-GA^-. The amplitude histogram (Figure 8) shows only the two peaks expected for the two symmetric, homodimeric channels. Upon the basis of the number of channels in each major peak in the histogram and a maximum of 2% of heterodimeric channels (see legend to Figure 8), we estimate that less than 2.5% of the Gly_{15}-GA subunits could have folded as left-handed $\beta^{6.3}$ helices (cf. ref *73*). Therefore, it can be concluded that the Trp → Gly substitution at position 15 is of little consequence for the channel's folding, as could be deduced from the fact that Gly_{15}-GA forms channels as readily as the parent GA.

CONCLUSION

An analogue of GA has been synthesized in which the tryptophan residue at position 15 has been replaced by glycine. The Gly_{15}-GA analogue incorporated into SDS micelles forms a single helical species unlike the Ala_{15}-GA analogue that adopts multiple helical forms in SDS micelles (unpublished results). The removal of the tryptophan "anchor" (*74*) at the critical aqueous-micelle interface does not significantly alter the structure of the channel since the peptide backbone structure is not perturbed and only the orientation of Trp_{11} is altered relative to the parent GA channel. However, the removal of the tryptophan dipole at the channel entrance has a significant affect on the energetics and kinetics of cation binding and transport through the

Gly_{15}-GA channel. Thus, we conclude that the absence of ion−dipole interactions and, perhaps, aromatic side chain interactions with the interface, together with the change in orientation of the Trp_{11} side chain is responsible for the increased barrier for ion entry and exit from the channel. The changes in barrier height and well depth also will alter the alkali metal cation interactions with Tl^+ and may weaken cation binding.

SUPPORTING INFORMATION AVAILABLE

Chemical shifts for all ^1H in Gly_{15}-GA are provided as supplementary information. This material is available free of charge via the Internet at http://pubs.acs.org.

REFERENCES

1. Wallace, B. A, and Janes, R. W. (1999) in *Tryptophan, Serotonin and Melatonin*: *Basic Aspects and Applications* (G. Huether, Ed.) p 789, Kluwer Academic/Plenum Publishers, New York.
2. Schiffer, M., Chang, C.-H., and Stevens, F. J. (1992) *Protein Eng. 5*, 213.
3. Wallace, B. A. (2000) *BioEssays 22*, 227.
4. Hinton, J. F. (1999) in *Annual Reports in NMR Spectroscopy* (Webb, G. A., Ed.), Vol. 38, Chapter 2, Academic Press, London.
5. Townsley, L. E., Tucker, W. A., Sham, S., and Hinton, J. F. (2001) *Biochemistry 40*, 11676.
6. Urry, D. W. (1972) *Biochim. Biophys. Acta 265*, 115.
7. Sarges, R., and Witkop, B. (1965) *J. Am. Chem. Soc. 87*, 2011.
8. Urry, D. W. (1971) *Proc. Natl. Acad. Sci. U.S.A. 68*, 672.
9. Weinstein, S., Wallace, B. A., Blout, E. R., Morrow, J. S., and Veatch, W. R. (1979) *Proc. Natl. Acad. Sci. U.S.A. 76*, 4230.
10. Wallace, B. A. (1996) in *Recent Advances in Tryptophan Research* (Filippini, G. A., et al., Eds.) p 607, Plenum Press, New York.
11. Williams, L. P., Narcesian, E. J., Andersen, O. S., Waller, G. R., Taylor, J., Lazenby, J. R., Hinton, J. F., and Koeppe, R. E., II. (1992) *Biochemistry 31*, 7311.
12. Mazet, J.-L., Andersen, O. S., and Koeppe, R. E., II (1984) *Biophys. J. 45*, 263.
13. Hinton, J. F., Fernandez, J. Q., Shungu, D., and Millet, F. S. (1989) *Biophys. J. 55*, 327.
14. Hinton, J. F., Fernandez, J. Q., Shungu, D., Whaley, W. L., Koeppe, R. E., II, and Millett, F. S. (1988) *Biophys. J. 53*, 145.
15. Hinton, J. F., Koeppe, R. E., II., Shungu, D., Whaley, W. L., Paczkowski, J. A., and Millett, F. S. (1986) *Biophys. J. 49*, 571.
16. Hinton, J. F., Newkirk, D. K., and Fletcher, T. G. (1994) *J. Magn. Reson., Ser. B 105*, 11.
17. Urry, D. W., Spisni, A., and Khaled, M. A. (1979) *Biochem. Biophys. Res. Commun. 88*, 940.
18. Spisni, A., Khaled, M. A., and Urry, D. W. (1979) *FEBS Lett. 102*, 321.
19. Hinton, J. F., Young, G., and Millett F. S. (1982) *Biochemistry 21*, 651.
20. Hinton, J. F., Whaley, W. L., Shungu, D. C. Koeppe, R. E., II., and Millett F. S. (1986) *Biophys. J. 50*, 539.
21. Lauger, P. (1985) *Angew. Chem., Int. Ed. Engl. 24*, 905.
22. Stark, G., and Benz, R. (1971) *J. Membr. Biol. 5*, 133.
23. Urry, D. W., Spisni, A., Khaled, M. A., Long, M. M., and Masotti, L. (1979) *Int. J. Quantum Chem., Quantum Biol. Symp. 6*, 289.
24. Urry, D. W., Trapane, T. L., and Prasad, K. U. (1983) *Science 221*, 1064.
25. Masotti, L., Spisni, A., and Urry, D. W. (1980) *Cell. Biophys. 2*, 241.
26. Gupta, R. K., and Gupta, P. (1982) *J. Magn. Reson. 47*, 34.
27. Pike, M. M., Simon, S. R., Balschi, J. A., and Springer, C. S. (1982) *Proc. Natl. Acad. Sci. U.S.A. 79*, 810.
28. Chu, S., Pike, M. M., Fossel, E. T., Smith, T. W., Balschi, J. A., and Springer, C. S. (1984) *J. Magn. Reson. 56*, 33.
29. Szoka, F., and Papahadjopoulos, D. (1978) *Proc. Natl. Acad. Sci. U.S.A. 75*, 4194.
30. Buster, D. C., Hinton, J. F., Millett, F. S., and Shungu, D. C. (1988) *Biophys. J. 53*, 145.
31. Hinton, J. F., Easton, P. L., Newkirk, D. K., and Shungu, D. C. (1993) *Biochim. Biophys. Acta 146*, 191.
32. Hinton, J. F., Jordan, J. B., and Horne, E. (2001) *J. Mol. Struct. 602*, 251.
33. Hinton, J. F., and Washburn, A. M. (1995) *Biophys. J. 69*, 435.
34. Hinton, J. F., Washburn, A. M., Snow, A., and Douglas, J. (1997) *J. Magn. Reson. 124*, 132.
35. Wüthrich, K. (1986) *NMR of Proteins and Nucleic Acids*, John Wiley and Sons, New York.
36. Bodenhausen, G., Kogler, H., and Ernst, R. R. (1984) *J. Magn. Reson. 58*, 370.
37. States, D. J., Haberkorn, R. A., and Ruben, D. J. (1982) *J. Magn. Reson. 48*, 286.
38. Bax, A., and Davis, D. G. (1985) *J. Magn. Reson. 65*, 355.
39. Hinton, J. F., Metz, K. R., and Briggs, R. W. (1988) in *Progress in Nuclear Magnetic Resonance Spectroscopy* (Webb, G. A., Ed.) Vol. 20, p 423, Pergamon Press, New York.
40. Forsén, S., and Hoffman, R. A. (1966) *J. Chem. Phys. 45*, 2049.
41. Alger, J. R., and Shulman, R. G. (1984) *Q. Rev. Biophys. 17*, 83.
42. Alger, J. R., and Prestegard, J. H. (1979) *Biophys. J. 28*, 1.
43. Ridell, F. G., Arumugam, S., and Patel, A. (1990) *Inorg. Chem. 29*, 2398.
44. Ridell, F. G., and Arumugam, S. (1989) *Biochim. Biophys. Acta 984*, 6.
45. Ridell, F. G., and Hayer, M. K. (1985) *Biochim. Biophys. Acta 817*, 31.
46. Ridell, F. G., and Arumugam, S. (1988) *Biochim. Biophys. Acta 945*, 65.
47. Ridell, F. G., Arumugam, S., and Cox, B. G. (1987) *J. Chem. Soc., Chem. Commun.* 1890.
48. Forsén, S., and Hoffman, R. A. (1963) *J. Chem. Phys. 39*, 2892.
49. Buster, D. C., Hinton, J. F., Millett, F. S., and Shungu, D. C. (1988) *Biophys. J. 53*, 145.
50. Shungu, D. C., and Briggs, R. W. (1988) *J. Magn. Reson. 77*, 491.
51. Shungu, D. C., Buster, D. C., and Briggs, R. W. (1990) *J. Magn. Reson. 89*, 102.
52. Robinson, G., Kuchel, P. W., Chapman, B. E., Dodrell, D. M., and Irving, M. G. (1987) *J. Magn. Reson. 63*, 314.
53. Muhandiram, D. R., and McClung R. E. D. (1987) *J. Magn. Reson. 71*, 187.
54. Vallazza, E., Bain, A. D., and Swaddle, T. W. (1988) *Can. J. Chem. 76*, 183.
55. Bain, A. D., and Cramer, J. A. (1993) *J. Magn. Reson., Ser. A 103*, 217.
56. Bain, A. D., and Cramer, J. A. (1993) *J. Phys. Chem. 97*, 2884.
57. Andersen, O. S. (1983) *Biophys. J. 4*, 119.
58. Sawyer, D. B., Koeppe, R. E., and Andersen, O. S. (1989) *Biochemistry 28*, 6571.
59. Durkin, J. T., Koeppe, R. E., and Andersen, O. S. (1990) *J. Mol. Bol. 211*, 221.
60. Andersen, O. S., and Procopio, J. (1980) *Acta Physiol. Scand. Suppl. 481*, 27.
61. Hinton, J. F. (1996) *J. Magn. Reson. 112*, 26.
62. Urry, D. W., Prasad, K. U., and Trapane, T. L. (1982) *Proc. Natl. Acad. Sci. U.S.A. 79*, 390.
63. Smith, R., Thomas, D. E., Atkins, A. R., Separovic, F., and Cornell, B. A. (1990) *Biochim. Biophys. Acta 1026*, 161.
64. Separovic, F., Gehrmann, J., Mile, T., and Cornell, B. A. (1994) *Biophys. J. 67*, 1495.
65. Becker, M. D., Greathouse, D. V., Koeppe, R. E., II., and Andersen, O. S. (1991) *Biochemistry 30*, 8830.
66. Andersen, O. S., Greathouse, D. V., Providence, L. L., Becker, M. D., and Koeppe, R. E., II. (1998) *J. Am. Chem. Soc. 120*, 5142.
67. Busath, D. D., Thulin, C. D., Hendershot, R. W., Phillips, L. R., Maughan, P., Cole, C. D., Bingham, N. C., Morrison, S., Baird, L. C., Hendershot, R. J., Cotton, M., and Cross, T. A. (1988) *Biophys. J. 75*, 2830.
68. Thompson, N., Thompson, G., Cole, C. D., Cotton, M., Cross, T. A., and Busath, D. D. (2001) *Biophys. J. 81*, 1245.
69. Anderson, D. G., Shirts, R. B., Cross, T. A., and Busath, D. D. (2001) *Biophys. J. 81*, 1255.
70. Dougherty, D. A. (1996) *Science 271*, 163.
71. Wimley, W. C., and White, S. H. (1992) *Biochemistry 31*, 12813.
72. Fonseca, V., Daumas, P., Ranjalahy-Rasoloarijao, L., Heitz, F., Lazaro, R., Trudelle, Y., and Andersen, O. S. (1992) *Biochemistry 31*, 5340.
73. Andersen, O. S., Saberwal, G., Greathouse, D. V., and Koeppe, R. E. (1996) *Ind. J. Biochem. Biophys. 33*, 331.
74. Koeppe, R. E., II., Killian, J. A., Greathouse, D. V., and Andersen, O. S. (1998) *Biol. Skr. − K. Dan. Vidensk. Selsk. 49*, 93.

BI0204286